RESEARCH REPORTS
Biomaterials & Bioengineering

P.A. Miguez[1], M. Terajima[1], H. Nagaoka[1], J.A.R. Ferreira[1], K. Braswell[1], C.C. Ko[2], and M. Yamauchi[1]*

[1]North Carolina Oral Health Institute, The University of North Carolina at Chapel Hill, USA; and [2]Department of Orthodontics, The University of North Carolina at Chapel Hill; *corresponding author, Mitsuo_Yamauchi@unc.edu

J Dent Res 93(4):406-411, 2014

Recombinant Biglycan Promotes Bone Morphogenetic Protein-induced Osteogenesis

ABSTRACT

The aim of this study was to determine the effects of glutathione-S-transferase-fused recombinant biglycan (GST-BGN) on craniofacial bone regeneration. We recently demonstrated a positive effect of tissue-derived BGN on bone morphogenetic protein 2 (BMP-2) function, which is exerted likely via the BGN core protein. Here, we investigated the effects of GST-BGN lacking any post-translational modifications on BMP-2 function *in vitro* and *in vivo*. In the C2C12 cell culture system, BMP-2-induced Smad 1/5/8 phosphorylation and alkaline phosphatase activity were both enhanced by the addition of GST-BGN. For the *in vivo* effect, we employed a Sprague-Dawley rat mandible defect model utilizing 1 μg (optimal) or 0.1 μg (suboptimal) of BMP-2 combined with 0, 2, 4, or 8 μg of GST-BGN. At 2 weeks post-surgery, newly formed bone was evaluated by microcomputed tomography and histologic analyses. The results revealed that the greatest amounts of bone within the defect were formed in the groups of suboptimal BMP-2 combined with 4 or 8 μg of GST-BGN. Also, bone was well organized versus that formed by the optimal dose of BMP. These results indicate that recombinant BGN is an efficient substrate to promote low-dose BMP-induced osteogenesis.

KEY WORDS: proteoglycan, growth factor, microcomputed tomography, critical-sized defect, Smad 1/5/8, bone regeneration.

DOI: 10.1177/0022034514521237

Received July 9, 2013; Last revision December 26, 2013; Accepted January 3, 2014

INTRODUCTION

Bone defects of congenital and acquired origins are a major health concern to our society, directly affecting the quality and length of life. To regenerate bone, an approach of tissue engineering has been developed consisting of a biocompatible scaffold, osteogenic growth factors such as bone morphogenetic proteins (BMPs), and stem cells. Yet, the clinical use of BMPs faces challenges such as high cost because of the high quantities of BMP required, the difficulties to retain BMP *in situ*, and a robust post-operative inflammatory response (Selvig *et al.*, 2002; Smucker *et al.*, 2006; Dickerman *et al.*, 2007).

Biglycan (BGN), a member of class I molecules in the small leucine-rich proteoglycan family, is one of the major noncollagenous proteins in mineralized tissues (Fisher *et al.*, 1983). It may function as nucleator for mineral deposition in an *in vitro* system (Boskey *et al.*, 1997) and/or modulator of osteoblast and chondroblast activities (Bianco *et al.*, 1990). It also has been shown that BGN is a positive modulator of BMP function and promotes osteoblast differentiation and mineralization (Chen *et al.*, 2004; Parisuthiman *et al.*, 2005). More recently, using tissue-derived BGN, we demonstrated that this function is likely exerted through the core protein and that the glycosaminoglycan (GAG) rather functions as a suppressor (Miguez *et al.*, 2011).

Thus, to explore the potential utility of recombinant BGN for BMP-2-induced osteogenesis, we investigated the effect of glutathione-S-transferase-fused BGN (GST-BGN) devoid of the posttranslational modifications including GAGs and N-glycosylation. Our study characterizes the effects of GST-BGN on BMP signaling and functions by the C2C12 cell assay system and then tests the effect of GST-BGN on BMP-2-induced early osteogenesis in a rat mandible defect model. The hypothesis tested was that GST-BGN is a potent BMP-2 function promoter *in vitro* and *in vivo*, leading to predictable bone regeneration.

MATERIALS & METHODS

Cell Culture

C2C12 cells were cultured as previously described (Mochida *et al.*, 2006). Briefly, cells were grown in DMEM (Invitrogen, Carlsbad, CA, USA) with high glucose (4.5 g/L) containing 15% FBS (Invitrogen) and supplemented with 100 U/mL of penicillin G sodium and 100 μg/mL of streptomycin sulfate.

Generation of Recombinant BGN and Verification of Effect on BMP-2 Function

Recombinant BGN fused with GST tag was generated in an *Escherichia coli* system and purified as previously reported (Mochida *et al.*, 2006). The purity of GST-BGN was assessed by 4% to 12% SDS-PAGE stained with CBB and

Western blot (WB) with anti-GST antibody (Sigma-Aldrich, St Louis, MO, USA). The effect of GST-BGN on rBMP-2 function (R&D, Minneapolis, MN) was confirmed by alkaline phosphatase (ALP) activity as described elsewhere (Kaku *et al.*, 2007). Briefly, after 4 days of culture, cell/matrix was lysed with Tris buffer saline containing 0.1% Triton X. ALP activity was measured with ALP yellow (pNPP; *p*-nitrophenylphosphate) Liquid Substrate System for ELISA (Sigma, St. Louis, MO, USA) according to the manufacturer's protocol. The pNP production was measured by absorbance at 405 nm via a 96-well plate reader. The protein concentration was determined by a DC Protein Assay kit (Bio-Rad, Hercules, CA, USA) and ALP activity calculated as mol of pNP/min/total protein. A one-way analysis of variance was conducted for the variable "treatment" at 95% confidence interval ($n = 3$). The dose effect of GST-BGN on BMP-2 signaling was evaluated by adding 2, 4, or 8 μg of GST-BGN (based on previous pilot experiments showing no effect of BGN at higher concentrations than 8 μg) combined with 150 ng per 2 mL of BMP-2 to C2C12 cells, followed by the measurement of phosphorylation of Smad 1/5/8. Both experiments were done at least in triplicates.

Smad 1/5/8, β-catenin, and ERK 1/2 Phosphorylation

The effects of GST-BGN on Smad and non-Smad BMP-2 signaling pathways were assessed by the phosphorylation of Smad1/5/8, β-catenin, and ERK 1/2 in C2C12 cells. Briefly, cells were treated with 4 μg of GST-BGN and 150 ng of BMP-2 for 1 hr and extracted with RIPA buffer. The extracts were then applied to 4% to 12% SDS-PAGE followed by WB analyses with anti-phospho (*p*)–Smad 1/5/8, anti-*p*-β-catenin antibody, or anti-*p*-ERK 1/2 (Cell Signaling, Danvers, MA, USA). Levels were normalized to β-actin and β-catenin (cell signaling).

Animal Surgery

The surgical procedures were performed as previously described (Zellin and Linde, 1997; Miguez *et al.*, 2011). Briefly, 5-mm critical-sized defects were generated in mandibles of Sprague-Dawley male rats via a trephine bur. A collagen scaffold loaded with or without proteins was placed within the defect, and bone regeneration was evaluated at 2 wk postsurgery. Animal experiments were approved by the Institutional Animal Care and Use Committee (ID 09-237.0) at the University of North Carolina at Chapel Hill and conform to the ARRIVE guidelines. According to Arosarena and Collins (2005), 0.1 μg of BMP-2 is considered a "suboptimal" dose of BMP in this model because defects exhibit minimal osteogenesis, whereas 1 μg is an "optimal" dose to promote accelerated and increased bone regeneration of the mandible. Thus, the suboptimal dose of BMP (subBMP) was used to evaluate the effect of GST-BGN on BMP-induced bone formation. The optimal dose of BMP (optBMP) was used for comparison of the amount and organic matrix quality of bone formed to those of subBMP with and without BGN. Control groups included (1) unfilled defect, (2) collagen scaffold alone (Nitta Gelatin Inc, Osaka, Japan), (3) collagen scaffold filled with 4 μg of GST-BGN, and (4) collagen scaffold filled with 4 μg of GST protein alone (*i.e.*, a total of 4 control groups without addition of subBMP). Treatment groups received the scaffold loaded with (5) subBMP alone or combined with (6) 2 μg of GST-BGN, (7) 4 μg of GST-BGN, or (8) 8 μg of GST-BGN and (9) optBMP (*i.e.*, a total of 5 treatment groups). Rats were euthanized as described (Miguez *et al.*, 2011). Three animals per group were implanted for 2 wk, as the optimal dose of BMP-2 has been shown to promote closure of such mandible defect around this time point (Zellin and Linde, 1997).

Microcomputed Tomography

The mandibles were fixed in 10% formalin and subjected to microcomputed tomography (μCT) analysis via the Scanco Medical μCT (Skyscan, Belgium) as previously described (Miguez *et al.*, 2011). Bone volume (BV) was determined as BV/total area of the newly formed bone (NFB).

Histologic Analyses

Mandibles were demineralized with 0.5 M EDTA, pH 7.4, for 8 wk, dehydrated, and embedded in paraffin. Sections (6 μm) obtained from the mid–cross section of the mandible defects were stained by Masson's trichrome for histomorphometry or by picrosirius red (PSR) to evaluate collagen organization and maturation (Junqueira *et al.*, 1979). Osteoclastic activity was analyzed by tartrate-resistant acid phosphatase (TRAP) (Yan *et al.*, 2007).

RESULTS

Effect of GST-BGN on BMP-2 Signaling and Function *In Vitro*

Figure 1A shows SDS-PAGE stained with CBB for the newly generated GST-BGN and GST, revealing the single bands at the expected migration positions at ~70 kDa (45 kDa BGN core + ~26 kDa GST) and ~26 kDa, respectively. WB analysis confirmed that both were immunopositive against anti-GST antibody (not shown). The statistically significant positive effect of GST-BGN on BMP-2-induced ALP activity was observed (lane 6) compared to BMP-2 alone (lane 4) or BMP-2 + GST (lane 5) (Figure 1B), which is consistent with a previous report (Mochida *et al.*, 2006). The Smad 1/5/8 phosphorylation (Figure 1C) was induced with BMP-2 (lanes 1, 2) and enhanced with the addition of 2 μg of GST-BGN (lane 3). Phosphorylation was further increased with 4 μg of GST-BGN (lane 4) and stayed at a similar level with 8 μg (lane 5).

Figure 1D shows the comparison of Smad and non-Smad signaling in C2C12 cells induced by BMP-2 with and without 4 μg of GST-BGN. Smad 1/5/8 phosphorylation was enhanced by GST-BGN in BMP-2-treated C2C12 cells (upper panel); β-catenin phosphorylation did not change with BMP-2 in the presence or absence of GST-BGN (middle panel) when normalized to total β-catenin. ERK 1/2 phosphorylation was reduced with BMP-2 (lane 2), and the addition of GST-BGN (lane 3) had no apparent effect. In all these *in vitro* experiments, GST-BGN never exerted any effect by itself at any dose tested, and this was observed in repeated experiments with the same GST-BGN or with different batches of this bacteria-generated protein.

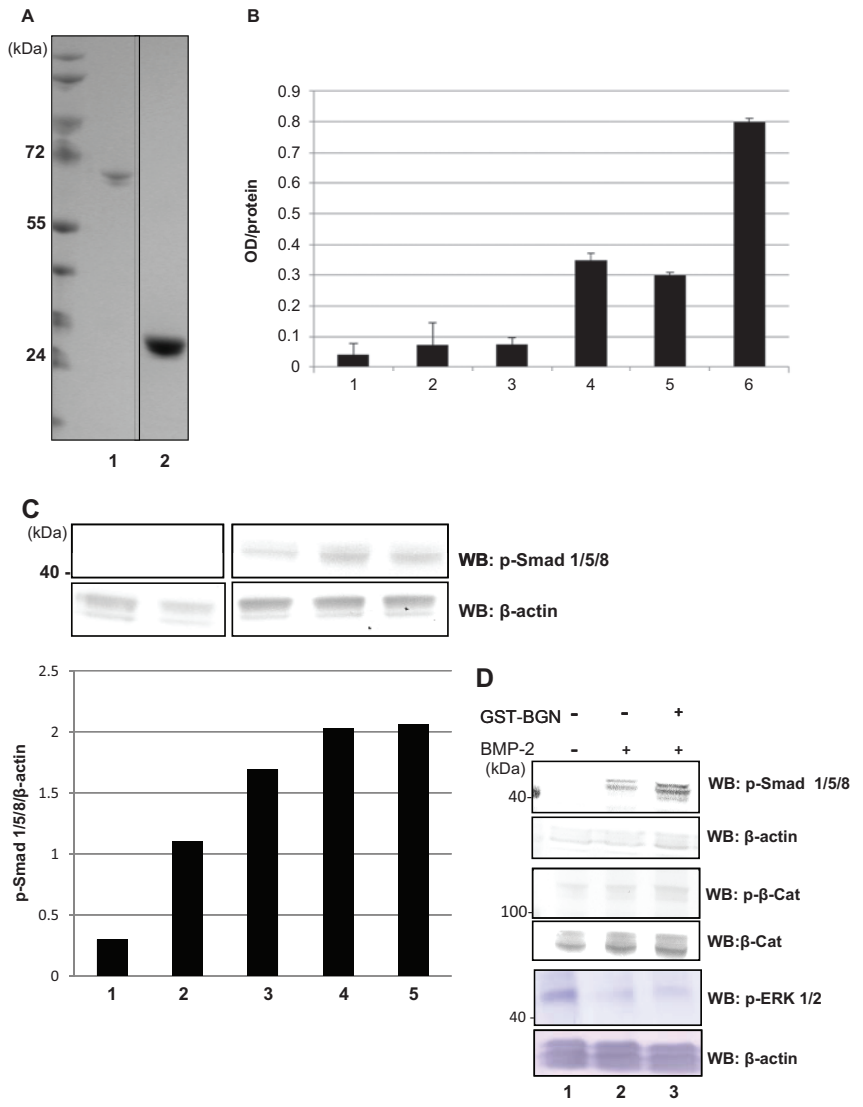

Figure 1. **(A)** SDS-PAGE analysis of glutathione-S-transferase-fused biglycan (GST-BGN) and GST protein. Molecular weight markers are shown at the very left lane. By SDS-PAGE stained with Coomassie Brilliant Blue, GST-BGN migrates at ~70 kDA (lane 1) and GST at about 26 kDA (lane 2). **(B)** Alkaline phosphatase (ALP) activity in C2C12 cells (n = 3). Lane 1, no treatment; lane 2, GST alone; lane 3, GST-BGN; lane 4, BMP-2 (150 ng); lane 5, BMP-2 + GST; lane 6, BMP-2 + GST-BGN. Note that GST-BGN significantly increased BMP-2-induced ALP activity in C2C12. **(C)** Dose effect of GST-BGN on BMP-2 signaling evaluated by Smad1/5/8 phosphorylation (n = 3). One representative membrane is shown. Upper panel, Western blot analysis; lower panel, Smad1/5/8 phosphorylation normalized to β-actin based on the Western blot analysis (densitometry by Scion Image Software, Scion Corporation). Lane 1, no treatment; lane 2, BMP-2; lane 3, BMP-2 + 2 μg GST-BGN; lane 4, BMP-2 + 4 μg of GST-BGN; lane 5, BMP-2 + 8 μg of GST-BGN. Note that 2 μg of GST-BGN increased phosphorylation of Smad 1/5/8 (lane 3), as did 4 μg (lane 4), yet 8 μg maintained its level (lane 5). **(D)** Signaling pathways upon BMP-2 and BMP-2 + GST-BGN treatments. Note that GST-BGN enhanced BMP-2-induced Smad phosphorylation (upper panel, lane 3). No increase in p-β-catenin is seen with any of the treatments (middle panel) after normalization to β-catenin. Lower panel shows that BMP-2 reduced p-Erk 1/2 (lane 2), and lane 3 indicates that addition of GST-BGN did not change the effect.

Tomographic BV of the NFB in the Rat Mandibles

Figure 2 shows the representative 3-dimensional (upper panel) and 2-dimensional (middle panel) μCT images and BV (lower panel). The BV values of control groups—that is, unfilled, scaffold alone, scaffold + GST-BGN, scaffold + GST (not shown)—were not statistically significantly different from that of subBMP (lane 1). Compared with these groups, the amounts of NFB were significantly higher in the optBMP group (lane 2). However, the bone induced by optBMP appeared to be mainly ectopic (see its 2-dimensional image in the middle panel), and less than 80% of the defect area was filled with NFB (defect area identified by upper and lower edges of native bone). Addition of 2 μg of GST-BGN to subBMP-2 (lane 3) did not significantly enhance bone formation compared to that of subBMP-2 alone. However, when subBMP was combined with 4 or 8 μg of GST-BGN, a significant increase in bone formation was observed (lanes 4 and 5, respectively), and the means were similar to optBMP (Wilcoxon rank sum, $p > .05$).

BV was calculated by the μCT software CTan Analyzer (Skyscan, Kontich, Belgium).

Histologic Evaluation

In control groups, there was minimal NFB at the edge of the defect; thus, not all the histologic images are shown. In Figure 2, for ease of identification, the edge of the NFB is delineated by a dotted yellow line and the native bone by a solid line. The subBMP group showed a small amount of NFB (Figure 2B) compared to the scaffold-only group (Figure 2A), while the optBMP group showed a much greater amount of NFB (Figure 2C). Figure 2D, E, and F show the images obtained from the subBMP groups combined with 2, 4, or 8 μg of GST-BGN, respectively. While NFB/total area percentage did not change with the addition of 2 μg of GST-BGN to subBMP (15.5 ± 2) (Figure 2D) compared to that of subBMP alone (8.3 ± 4.2), it increased with 4 μg (Figure 2E) and 8 μg of GST-BGN (Figure 2F).

PSR staining shown in Figure 3A (4×) and B (40×) demonstrates the collagen matrices of the NFB in the subBMP group are well organized and mature as indicated by the intense red staining of the collagen fibers. The NFB of the optBMP group showed light yellow to red color with patches of green color, indicating that the collagen matrix is less mature and less organized (Figure

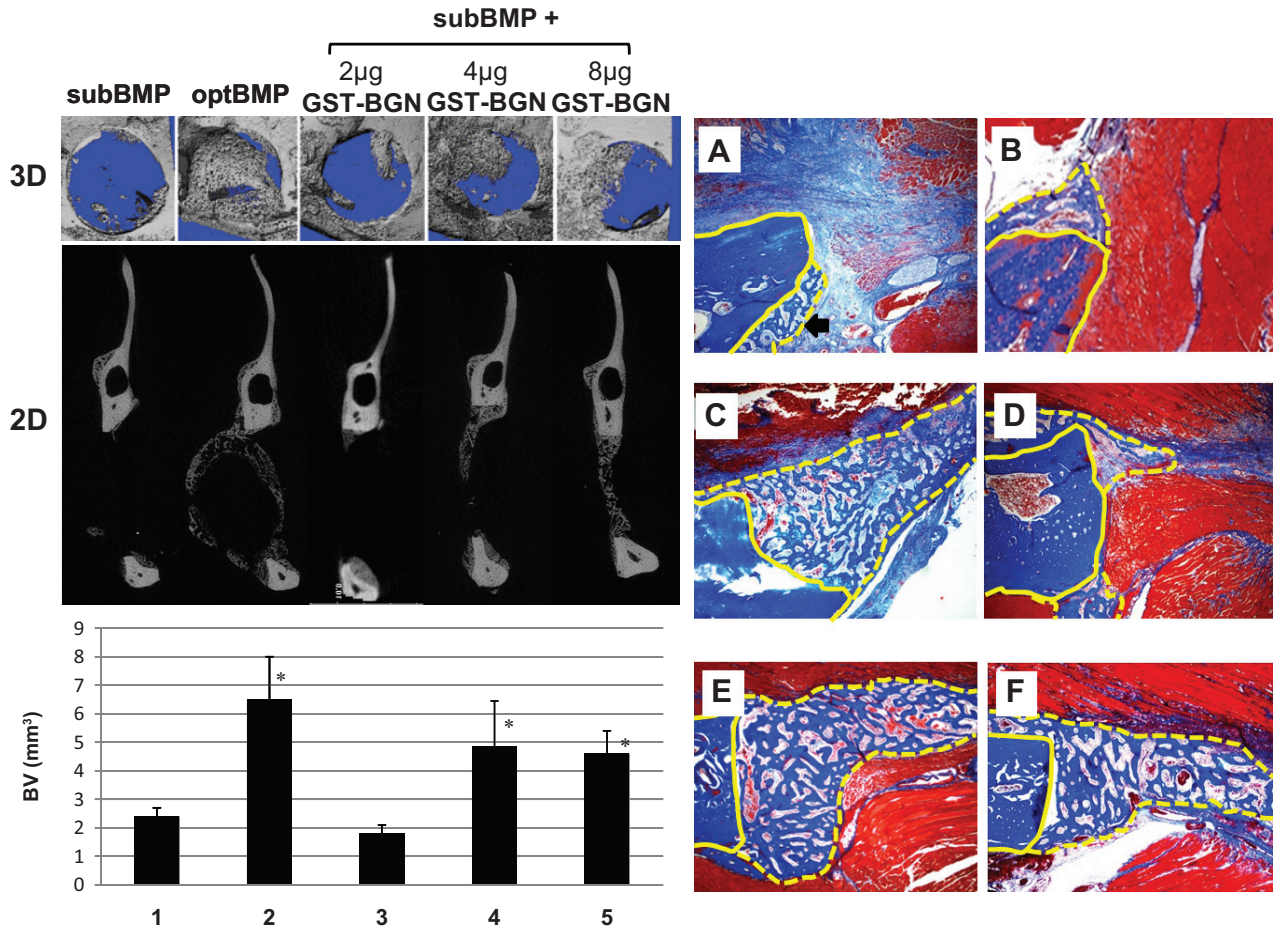

Figure 2. Microcomputed tomography and histologic analyses of the rat mandibles showing 3-dimensional (upper panel) and 2-dimensional (middle panel) views of the mandibles. Lower panel shows the bone volume (BV) quantitated by computed tomography analyzer software. Data were expressed as bars (means ± standard deviation) and the statistical differences analyzed by Wilcoxon rank sum test to assess the average difference between conditions. Note that optBMP (lane 2) shows a tendency of greater BV but is mainly of ectopic nature. The newly formed bone by the subBMP + GST-BGN group is seen primarily within the defect (lanes 4 and 5), and BV is similar to optBMP (lane 2). Right panel shows Masson's trichrome staining of **(A)** scaffold alone (arrow: induction of newly formed bone [NFB] due to periosteum release), **(B)** subBMP, **(C)** optBMP, **(D)** subBMP + 2 μg GST-BGN, **(E)** subBMP + 4 μg GST-BGN, **(F)** subBMP + 8 μg of GST-BGN. Yellow solid line denotes native bone and yellow dotted line NFB. The total area (TA) of the defect was outlined using Image J (National Institutes of Health, Bethesda, MD, USA).

3C); upon higher magnification (Figure 3D), the coloration was more faint possibly, indicating a thinner collagen matrix. The subBMP + 4 μg and subBMP + 8 μg (Figure 3E) groups revealed more red, dense, and thick collagen fibers than those of optBMP alone (Figure 3C), as represented by stronger red signaling, although there was some green and yellow scattered patches (Dayan *et al.*, 1989). Thus, the use of GST-BGN did not compromise the collagen matrix organization/quality as the optBMP group did.

TRAP-positive staining was observed only in the optBMP group (Figure 4A). In these sections, the TRAP-positive cells were found mostly at the surface of the NFB (Figure 4A). Figure 4B shows a representative image of subBMP + 4 μg GST-BGN showing no TRAP-positive cells. Quantification is shown in Figure 4C.

DISCUSSION

Recently, we reported that the positive effect of tissue-derived BGN on BMP-2 function was likely exerted through its core protein (Miguez *et al.*, 2011). In the current study, we tested the utility of recombinant GST-BGN devoid of posttranslational modifications, including GAGs and N-glycosylation (Neame *et al.*, 1989). In the cell culture system, the positive effect was observed as previously reported (Mochida *et al.*, 2006). In the current study, the dose effect was examined and seen up to 4 μg of GST-BGN for 150 ng of BMP-2. The effect stayed at the same level with 8 μg of GST-BGN. Saturation of the ratio of GST-BGN to BMP and/or to its receptors may have limited further effect of GST-BGN on BMP function. Also, it is possible that while GST alone did not affect BMP function (Figure 1B),

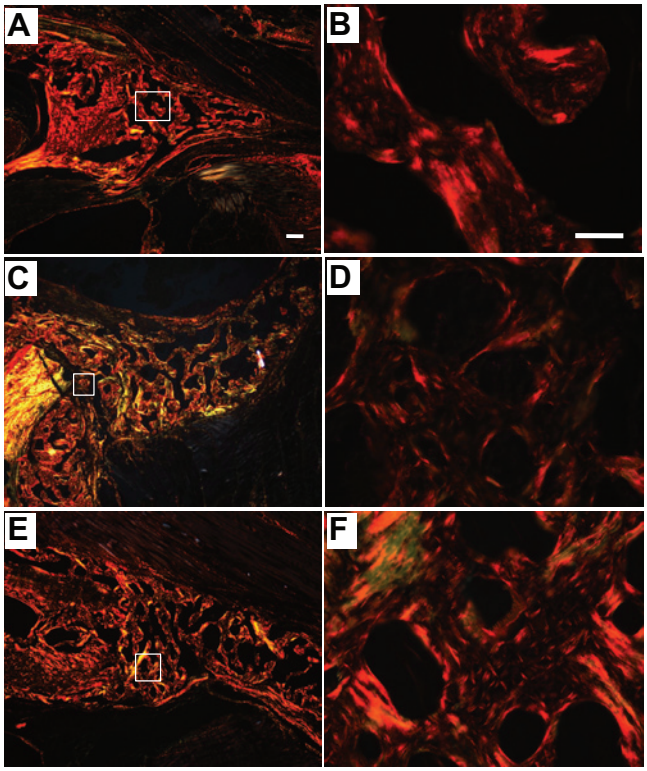

Figure 3. Picrosirius red staining of the newly formed bone areas. Polarized images of the NFB were taken from the areas immediately adjacent to the edge of the defects. **(A)** subBMP group showing collagen fibers in red color (4×), **(B)** high magnification of the boxed area in A (40×), **(C)** optBMP group showing collagen fibers in green/yellow to orange color (4×), **(D)** high magnification of the boxed area in C (40×), **(E)** the subBMP + 8 μg group showing collagen fibers in yellow to red color (4×), and **(F)** high magnification of the boxed area in E (40×). Scale bar is 500 μm in A and 200 μm in B.

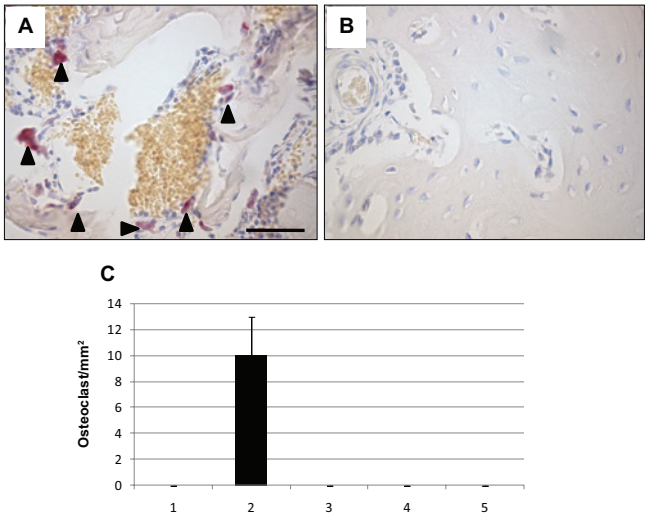

Figure 4. Tartrate-resistant acid phosphatase (TRAP) staining in the defects (40×): **(A)** optBMP, **(B)** subBMP + 4 μg, **(C)** number of osteoclast-like cells per mm^2. Lane 1, subBMP; lane 2, optBMP; lane 3, subBMP group + 2 μg GST-BGN; lane 4, subBMP + 4 μg; lane 5, subBMP + 8 μg. Trap-positive cells indicated by arrows were found in all rats treated with optBMP dose, while they were not detected in the subBMP with and without GST-BGN—thus, no bars shown in the figure. The number of osteoclast-like cells were counted as cells per mm^2 of NFB. Scale bar is 200 μm in A.

with high doses of GST-BGN, it potentially limits the BGN effect by interfering with the interaction between BMP-2 and its receptors.

Under the conditions used, positive effects were consistently seen for the Smad 1/5/8 pathway but were not observed for other signaling pathways, such as β-catenin and ERK 1/2, by the addition of BMP-2 or BMP-2 + GST-BGN. The reports on the effect of BMP on these signaling pathways are not consistent. Some studies showed that BMP-2 activates Wnt/β-catenin in C2C12, C3H10T1/2, and MC3T3-E1 cells (Rawadi *et al.*, 2003; Zhang *et al.*, 2009), while others reported the lack of such effect (Nakashima *et al.*, 2005). In a recent bone fracture–healing model, the callus of BGN-deficient mice reduced gene expression levels of Wnt-induced secreted protein 1, indicating a role of BGN in Wnt signaling (Berendsen *et al.*, 2011). The discrepancy between the current study and those reports could be due to the assay conditions, such as timing (1-hr incubation in this study), passage effect, and culture conditions, among others. There are also conflicting reports for the effect of BMP-2 on ERK signaling. Gallea *et al.* (2001) showed an increase of ERK phosphorylation with BMP-2 starting only at 2 hours' post-treatment in C2C12 cells, while Ghayor *et al.* (2009) reported a decrease in ERK signaling with BMP-2 treatment in C2C12 cells. These are likely due to the differences in the concentrations of BMP-2 and the timing of the assay. Kinetic studies of BMP-2 and BMP-2 + BGN downstream signaling pathways are warranted to identify the mechanisms by which BGN positively modulates the BMP-2 induced osteogenesis.

In the *in vivo* study, the NFB volume in the subBMP + 4 μg and subBMP + 8 μg groups was significantly greater than those of control groups and similar to that of optBMP (Figure 2, lower panel). The optBMP group, however, showed significant amounts of ectopic bone formation with limited amounts of bone bridging the defect. With excessive amounts of BMP-2, it could have led to extravasation of BMP to the surrounding tissues. Possibly, a greater amount of collagen per scaffold may help retain such large amounts of BMP-2. In addition, edema has been associated with large quantities of BMP-2 due to exacerbated inflammatory response (Shields *et al.*, 2006; Garrett *et al.*, 2010), which could contribute to extravasation of BMP to the surrounding connective tissues. Nonetheless, GST-BGN in combination with subBMP may provide a more predictable means of bone regeneration than optBMP, as the NFB was well confined to the defect boundaries. BGN has been shown to bind to collagen (Schonherr *et al.*, 1995) and BMPs (Mochida *et al.*, 2006). BGN may sequester BMP-2 to the extracellular matrix and thus both increase its potency and reduce negative effects such as edema.

Osteoclasts were identified only in the optBMP group. As reported, BMP-2 causes a dose- and time-dependent increase in

bone resorption pits excavated by osteoclasts and increases key enzymes for the degradation of bone matrices (Kaneko *et al.*, 2000), as supported by the pattern of PSR staining (Figure 3C and D). When collagen is resorbed and rapidly laid down, the formation of well-aligned mature collagen fibrils could be compromised.

In summary, this study accepted the hypothesis proposed and demonstrated the following: First, recombinant BGN devoid of posttranslational modifications specifically and predictably enhances BMP-2 function *in vitro* and *in vivo*; second, the bone formed by a low dose of BMP-2 combined with GST-BGN was well organized and mature when compared with that formed by a low or high dose of BMP-2 alone at 2 wk post-surgery; last, Smad pathway is consistently activated by BMP-2 and BGN-assisted BMP-2 osteogenesis *in vitro*. The data suggest that by utilizing a BMP-2 functional effector such as recombinant BGN, smaller quantities of BMP-2 could be used to possibly minimize adverse side effects, such as ectopic bone formation and robust inflammation (Shields *et al.*, 2006; Lee *et al.*, 2011; Zara *et al.*, 2011), and effectively regenerate craniofacial bone.

ACKNOWLEDGMENTS

The study was supported in part by the National Institutes of Health (grants R21 DE020909 and AR060978). The authors declare no potential conflicts of interest with respect to the authorship and/or publication of this article.

REFERENCES

Arosarena O, Collins W (2005). Comparison of BMP-2 and -4 for rat mandibular bone regeneration at various doses. *Orthod Craniofac Res* 8:267-276.

Berendsen AD, Fisher LW, Kilts TM, Owens RT, Robey PG, Gutkind JS, *et al*. (2011). Modulation of canonical Wnt signaling by the extracellular matrix component biglycan. *Proc Natl Acad Sci U S A* 108:17022-17027.

Bianco P, Fisher LW, Young MF, Termine JD, Robey PG (1990). Expression and localization of the two small proteoglycans biglycan and decorin in developing human skeletal and non-skeletal tissues. *J Histochem Cytochem* 38:1549-1563.

Boskey AL, Spevak L, Doty SB, Rosenberg L (1997). Effects of bone CS-proteoglycans, DS-decorin, and DS-biglycan on hydroxyapatite formation in a gelatin gel. *Calcif Tissue Int* 61:298-305.

Chen XD, Fisher LW, Robey PG, Young MF (2004). The small leucine-rich proteoglycan biglycan modulates BMP-4-induced osteoblast differentiation. *FASEB J* 18:948-958.

Dayan D, Hiss Y, Hirshberg A, Bubis JJ, Wolman M (1989). Are the polarization colors of picrosirius red-stained collagen determined only by the diameter of the fibers? *Histochemistry* 93:27-29.

Dickerman RD, Reynolds AS, Morgan BC, Tompkins J, Cattorini J, Bennett M (2007). rh-BMP-2 can be used safely in the cervical spine: dose and containment are the keys! *Spine J* 7:508-509.

Fisher LW, Termine JD, Dejter SW Jr, Whitson SW, Yanagishita M, Kimura JH, *et al*. (1983). Proteoglycans of developing bone. *J Biol Chem* 258:6588-6594.

Gallea S, Lallemand F, Atfi A, Rawadi G, Ramez V, Spinella-Jaegle S, *et al*. (2001). Activation of mitogen-activated protein kinase cascades is involved in regulation of bone morphogenetic protein-2-induced osteoblast differentiation in pluripotent C2C12 cells. *Bone* 28:491-498.

Garrett MP, Kakarla UK, Porter RW, Sonntag VK (2010). Formation of painful seroma and edema after the use of recombinant human bone morphogenetic protein-2 in posterolateral lumbar spine fusions. *Neurosurgery* 66:1044-1049.

Ghayor C, Ehrbar M, San Miguel B, Gratz KW, Weber FE (2009). cAMP enhances BMP2-signaling through PKA and MKP1-dependent mechanisms. *Biochem Biophys Res Commun* 381:247-252.

Junqueira LC, Bignolas G, Brentani RR (1979). Picrosirius staining plus polarization microscopy, a specific method for collagen detection in tissue sections. *Histochem J* 11:447-455.

Kaku M, Mochida Y, Atsawasuwan P, Parisuthiman D, Yamauchi M (2007). Post-translational modifications of collagen upon BMP-induced osteoblast differentiation. *Biochem Biophys Res Commun* 359:463-468.

Kaneko H, Arakawa T, Mano H, Kaneda T, Ogasawara A, Nakagawa M, *et al*. (2000). Direct stimulation of osteoclastic bone resorption by bone morphogenetic protein (BMP)-2 and expression of BMP receptors in mature osteoclasts. *Bone* 27:479-486.

Lee KB, Taghavi CE, Song KJ, Sintuu C, Yoo JH, Keorochana G, *et al*. (2011). Inflammatory characteristics of rhBMP-2 in vitro and in an in vivo rodent model. *Spine (Phila Pa 1976)* 36:E149-E154.

Miguez PA, Terajima M, Nagaoka H, Mochida Y, Yamauchi M (2011). Role of glycosaminoglycans of biglycan in BMP-2 signaling. *Biochem Biophys Res Commun* 405:262-266.

Mochida Y, Parisuthiman D, Yamauchi M (2006). Biglycan is a positive modulator of BMP-2 induced osteoblast differentiation. *Adv Exp Med Biol* 585:101-113.

Nakashima A, Katagiri T, Tamura M (2005). Cross-talk between Wnt and bone morphogenetic protein 2 (BMP-2) signaling in differentiation pathway of C2C12 myoblasts. *J Biol Chem* 280:37660-37668.

Neame PJ, Choi HU, Rosenberg LC (1989). The primary structure of the core protein of the small, leucine-rich proteoglycan (PG I) from bovine articular cartilage. *J Biol Chem* 264:8653-8661.

Parisuthiman D, Mochida Y, Duarte WR, Yamauchi M (2005). Biglycan modulates osteoblast differentiation and matrix mineralization. *J Bone Miner Res* 20:1878-1886.

Rawadi G, Vayssiere B, Dunn F, Baron R, Roman-Roman S (2003). BMP-2 controls alkaline phosphatase expression and osteoblast mineralization by a Wnt autocrine loop. *J Bone Miner Res* 18:1842-1853.

Schonherr E, Witsch-Prehm P, Harrach B, Robenek H, Rauterberg J, Kresse H (1995). Interaction of biglycan with type I collagen. *J Biol Chem* 270:2776-2783.

Selvig KA, Sorensen RG, Wozney JM, Wikesjo UM (2002). Bone repair following recombinant human bone morphogenetic protein-2 stimulated periodontal regeneration. *J Periodontol* 73:1020-1029.

Shields LB, Raque GH, Glassman SD, Campbell M, Vitaz T, Harpring J, *et al*. (2006). Adverse effects associated with high-dose recombinant human bone morphogenetic protein-2 use in anterior cervical spine fusion. *Spine (Phila Pa 1976)* 31:542-547.

Smucker JD, Rhee JM, Singh K, Yoon ST, Heller JG (2006). Increased swelling complications associated with off-label usage of rhBMP-2 in the anterior cervical spine. *Spine (Phila Pa 1976)* 31:2813-2819.

Yan D, Gurumurthy A, Wright M, Pfeiler TW, Loboa EG, Everett ET (2007). Genetic background influences fluoride's effects on osteoclastogenesis. *Bone* 41:1036-1044.

Zara JN, Siu RK, Zhang X, Shen J, Ngo R, Lee M, *et al*. (2011). High doses of bone morphogenetic protein 2 induce structurally abnormal bone and inflammation in vivo. *Tissue Eng Part A* 17:1389-1399.

Zellin G, Linde A (1997). Importance of delivery systems for growth-stimulatory factors in combination with osteopromotive membranes: an experimental study using rhBMP-2 in rat mandibular defects. *J Biomed Mater Res* 35:181-190.

Zhang M, Yan Y, Lim YB, Tang D, Xie R, Chen A, *et al*. (2009). BMP-2 modulates beta-catenin signaling through stimulation of Lrp5 expression and inhibition of beta-TrCP expression in osteoblasts. *J Cell Biochem* 108:896-905.